



the society for solid-state
and electrochemical
science and technology

Journal of The Electrochemical Society

Effect of Grain Refinement and Immersion Time on Morphology, Topography and Corrosion Resistance of CCC-Coated 7075 Al Alloy

Kourosh Shirvani and Sadegh Mastali

J. Electrochem. Soc. 2011, Volume 159, Issue 2, Pages C74-C79.
doi: 10.1149/2.038202jes

**Email alerting
service**

Receive free email alerts when new articles cite this article - sign up in the box at the top right corner of the article or [click here](#)

To subscribe to *Journal of The Electrochemical Society* go to:
<http://jes.ecsdl.org/subscriptions>



Effect of Grain Refinement and Immersion Time on Morphology, Topography and Corrosion Resistance of CCC-Coated 7075 Al Alloy

Kourosh Shirvani^z and Sadegh Mastali^z

Department of Advanced Materials & New Energies, Iranian Research Organization for Science and Technology, Tehran 15815-3538, Iran

Chromate conversion coatings (CCCs) were synthesized on AA7075 alloy. The effects of sodium saccharin as a grain refining agent (GRA) and coating time on the coating morphology, topography, and alloy corrosion resistance were studied in this work. Morphologies and topographies of CCCs were examined using optical, scanning electron and atomic force microscopes. The corrosion behaviour was evaluated using potentiodynamic polarization and electrochemical impedance spectroscopy in 0.5 M NaCl solution. Major decreases in both coating grain size and corrosion rate occur at a GRA concentration of 1 g/l. Coating roughness increased to a limited nano-scale extent with increasing immersion time.

© 2011 The Electrochemical Society. [DOI: 10.1149/2.038202jes] All rights reserved.

Manuscript submitted September 14, 2011; revised manuscript received October 31, 2011. Published December 16, 2011.

Hardened aluminium alloys are extensively used in aerospace industries because of their excellent mechanical properties such as toughness and high strength due to presence of second-phase particles in the alloys.¹ In alloy group of 7xxx, the primary alloying elements including Zn, Mg and sometimes Cu are used for age hardening and damage tolerance, but they form a range of second phase particles that make them sensitive to localized corrosion.² Applying protective conversion coatings onto the alloy surface is one approach to improve the environmental performance as well as to increase paint adhesion.³ Chromate coating is a extremely effective and widely-used type of conversion coating for high strength Al alloys in aerospace applications due to advantages such as like high corrosion resistance, good paint adhesion, low costs, simple application process and low dimensional changes.⁴⁻¹² A combination of pressures, including environmental regulations on the use and handling of chromates, increased service-life requirements of the fleet of airplanes, and the cost of preventive maintenance, has motivated aerospace industries to invest in efforts to find improved and environment-friendly methods of corrosion protection. A number of replacements for chromate coatings have been developed in recent years, but none are as effective at inhibiting corrosion, especially for the high-strength Al alloys.⁷ Therefore, it has been concluded that developing a better understanding of the mechanisms of aluminium corrosion and chromate inhibition is a top priority and a prerequisite for the development of a successful chromate replacement.

During the chromating of an aluminium alloy, the CCC grows irregularly with poor coverage especially at the grain boundaries and precipitates.⁹ More recently, CCC deposition has been suggested as a multi-step process, i.e., hydrolysis, condensation and polymerization. Commonly, CCC formation is described as a redox reaction between Al and chromate ions (dominant as $\text{Cr}_2\text{O}_7^{2-}$),¹³ and as a consequence, the metal converts into a non-metallic film at the surface.¹⁴ The redox reaction forms Cr^{3+} rapidly and makes Cr^{3+} hydroxides which condense and precipitate on the surface by polymerization in the solution. The condensation and polymerization continue in air, accompanied with dehydration during the drying period which is known as the coating ageing time.¹⁵ The dehydration reaction leads in turn to the development of shrinkage cracks extending down to the base metal over the coating surface.⁹ According to the MIL-C-5541E standard, CCCs are specified as either Class 1A or Class 3 with the primary difference being coating thickness. Class 1A is a thicker coating with brownish-yellow appearance and is intended to provide corrosion prevention and Class 3 is recommended when lower electrical resistance is required and can vary from clear to light yellow in colour.

Significant progress has been made in the understanding of protection mechanisms of CCCs, especially since late 1980s with the advance of analytical techniques. Several mechanisms including the bipolar membrane mechanism,¹⁶ self-healing,¹⁷ anodic and cathodic inhibition¹⁸ and blocking defects in the oxide film^{19,20} have been proposed to explain how CCCs protect the aluminium alloy against corrosion. Moreover, extensive studies have been conducted on the structure and compositions of CCCs on aluminium alloys^{4-6,21,22} and on the effect of ageing time as well as temperature and relative humidity of the ageing environment on the coating surface morphology.²³

However, there is no published work on the effect of a grain refining agent in the chromating bath on the surface morphology of the CCC-coated aluminium alloys and its subsequent influence on the alloy corrosion resistance. The present work aims to investigate the role of sodium saccharin on the morphology and topography of a CCC-coated 7075-T6 Al alloy. This research characterises the coatings formed on 7075-T6 alloy by means of optical microscopy, SEM and AFM observations. In addition, the effects of immersion time and sodium saccharin concentrations on the coating corrosion resistance have been presented and discussed in this paper. The results show that a very fine mud-crack morphology using sodium saccharin in the chromating solution for chromated Al alloy 7075, with improved corrosion resistance.

Experimental

Materials and Treatment.— Rolled 7075-T6 Al sheets ($5 \times 5 \times 0.1$ cm) were used as the substrate. The nominal composition of the alloy is presented in Table I. The T6 refers to a multistage heat treatment involving dissolution, quenching and ageing that results in the formation of fine precipitates which reinforce the alloy. Prior to chromating, all samples underwent the following surface preparation steps:

- Acetone cleaning for 5 min.
- Dipping in 25%wt NaOH solution at 25°C for 30 s, then rinsing with distilled water.
- Dipping in 10 g dm⁻³ H₂SO₄ (95–98%vol) + 20 g dm⁻³ H₃PO₄ (85%vol) solution at 60°C for 4 min, then rinsing with distilled water.

Table I. Chemical compositions of Al 7075 alloy (%wt).

Al	Ti	Zn	Cr	Mg	Cu	Mn	Fe	Si
Bal.	0.2	5.1–6.1	0.18–0.28	2.1–2.9	1.2–2	0.3	0.5	0.4

^z E-mail: shirvani@irost.org; sadegh.mastali@gmail.com

- (d) Dipping in 1:1 HNO₃ (65%vol)-water solution + 10 cm³ dm⁻³ HF at 25°C for 1 min, then rinsing with distilled water.
- (e) Treatment in a chromating solution containing CrO₃, K₃Fe(CN)₆, NaF and C₇H₄O₃NSNa for different immersion times. The coated surfaces were rinsed in distilled water and then dried in laboratory air for 24 h. More details for the chromating procedure are presented elsewhere.²⁴ Sodium saccharin (C₇H₄O₃NSNa. 2H₂O) as grain refining agent (GRA, hereinafter) in different concentrations of 0, 0.5, 1 and 1.5 g/l was utilized in the chromating solution for evaluating the effect of the GRA concentration on coating morphology and corrosion resistance of the CCC-coated 7075 alloy.

Coating weight measurement.— To determine the weight of the CCC, coated samples were dried and weighed using a laboratory scale having ±0.0001 g resolution. Then the samples were immersed into a solution of 10 g dm⁻³ HNO₃ (65%vol) at 90°C for few seconds, rinsed and dried completely. This results in removing the formed CCC from the sample surface. The next step was re-weighing the samples. The weight of formed coating was calculated as follow:

$$W_C = W_1 - W_2 \quad (\text{in mg}) \quad [1]$$

W₁: weight of coated sample; W₂: weight of sample after the coating removal.

To improve the experimental data reproducibility, three samples of each conversion treatment time were tested.

Metallographic examinations.— The surface morphologies of the coatings were examined by means of an optical microscope and a JEOL JSM-T80 Scanning Electron Microscope (SEM) at accelerating voltage of 20 keV. The sample surface was covered with a very thin gold layer to reduce surface charging during examination in the electron microscope caused by the poorly conductive CCC.

The surface topography of the chromated samples was characterised using a Digital Instruments Nanoscope III Atomic Force Microscope (AFM). All measurements were carried out with non-contact tips. The scan area was 5 × 5 μm². Then, 3D-AFM images were analysed by WSXM-4 software to obtain roughness information from the CCC surface. Roughness command calculates several roughness parameters, such as the average of all the height (z) values within the enclosed area, the standard deviation of the z values (RMS), and the mean value of the surface relative to the centre plane (Ra).

Corrosion tests.— The corrosion resistance of the CCC-coated samples was assessed by potentiodynamic polarization tests and electrochemical impedance spectroscopy (EIS) in 0.5 M NaCl solution at room temperature. A conventional three-compartment cell was used for the electrochemical investigation. A sample of defined area 2 cm² as the working electrode was exposed to the test solution and all the current values were normalized to the geometrical surface area. A Pt sheet was used as the counter electrode; the reference electrode was a saturated calomel electrode (SCE).

For the potentiodynamic sweep experiments, the samples were first immersed into 0.5 M NaCl for about 10 min to stabilize the open-circuit potential E₀. Subsequently, potentiodynamic curves were recorded by sweeping the electrode potential from -50 mV to +600 mV (both with respect to E₀) at a sweep rate of 0.5 mV/s. EIS measurements were conducted at the open-circuit potential with applied 10 mV sinusoidal perturbations in the frequency range of 10⁴–10⁻¹ Hz. EIS data were evaluated by equivalent circuit modelling. A Princeton Applied Research (PAR) 273A potentiostat and Solartron 1266 frequency response analyser with Zplot™ software were used to evaluate the measurements.

Results and Discussion

Coating appearance and weight.— Observations after the conversion treatment for various immersion times illustrated that the coating colour varied from clear yellow to iridescent yellow and finally

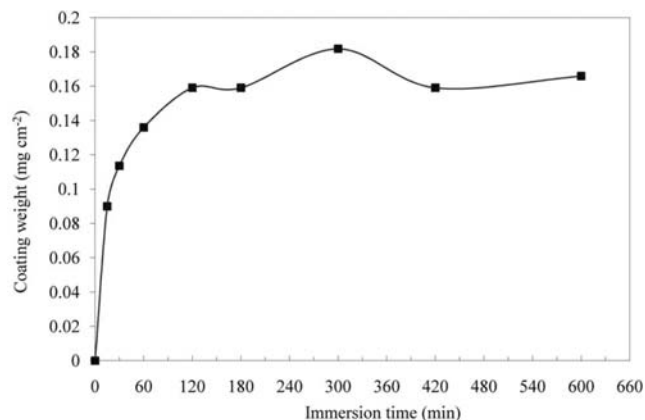


Figure 1. weight variation of the CCC-coated 7075 alloy treated with different immersion time.

to brownish yellow with increasing immersion time. As variegated colours are due mainly to interference colours for the thinner films and to the presence of chromium compounds in the film,²⁵ the coating thickness/weight plays a pivotal role on the CCC appearance. Figure 1 illustrates the weight of CCC as a function of the immersion time in the chromating bath. In agreement with results reported in the literature,²⁶ the samples show a very rapid formation of the chromate coating (about 0.006 mg s⁻¹) during the first 15 s. Afterwards, the coating weight increases slowly upon thickening of the layer on the surface.²⁶ Finally, the coating weight leveled off because of a balance between coating deposition and the substrate/coating dissolution processes.

Coating morphology and topography.— The dependence of the coating surface morphology (form and size of surface grains) on the GRA concentration and the effect of the immersion time on the coating surface topography (coating roughness) were investigated. Surface morphology observations by SEM demonstrated a mud-crack pattern for the surface of CCC-coated 7075 alloy as shown in Fig. 2. This familiar mud-crack morphology has been reported by several authors.^{4,27,28} The appearance suggests that the cracking is due

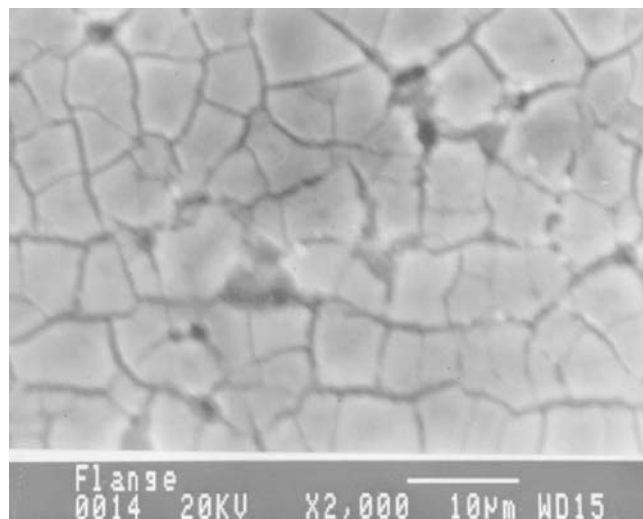


Figure 2. Secondary electron micrographs of the Mud-cracking morphology of CCC-coated 7075 alloy, immersion time: 30 s.

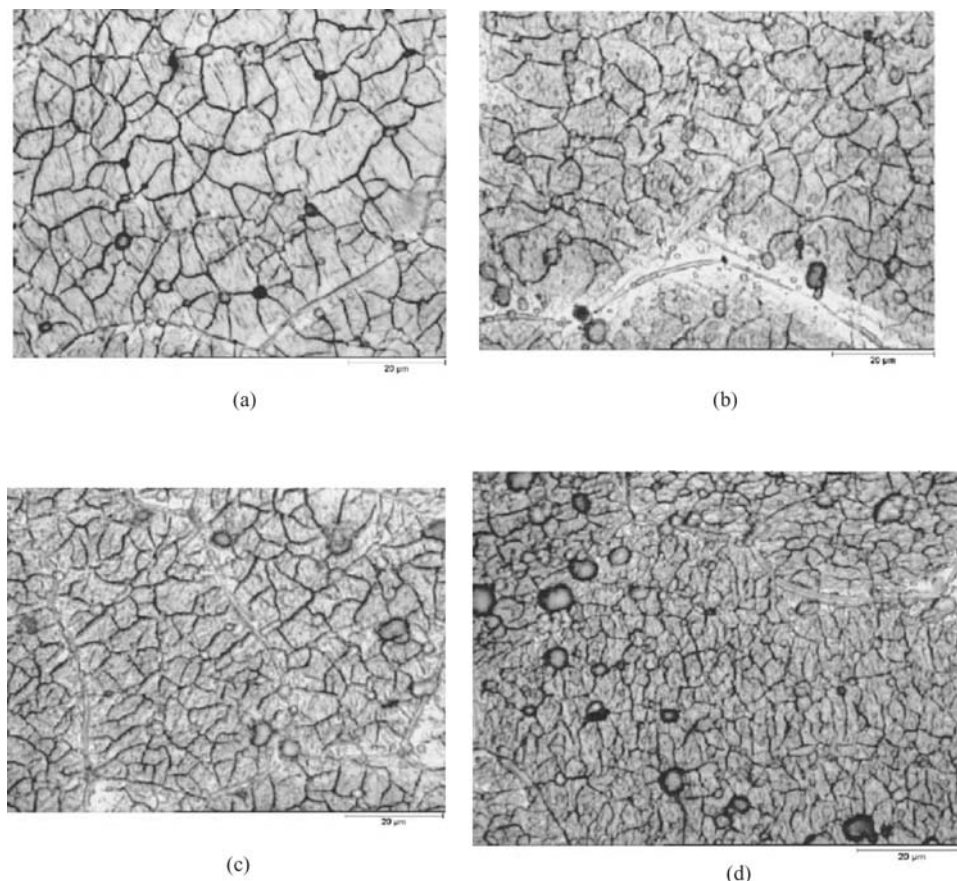


Figure 3. Optical micrographs of CCCs on the 7075 alloys obtained from different sodium saccharin concentrations (a) 0 g/l, (b) 0.5 g/l, (c) 1 g/l and (d) 1.5 g/l.

to shrinkage during coating drying. During differential dehydration across the coating thickness, a tensile stress parallel to the coating surface is developed and this stress causes shrinkage cracking in CCCs.²⁹ This type of surface structure plays an important role in the promotion of paint adhesion.^{30,31} According to an earlier study²⁴ the cracks become wider and deeper upon increasing the immersion time. This should be considered when developing a CCC for promoting the adhesion of superposed paint.

Effect of GRA on surface morphology.—To evaluate the GRA effect on the coating morphology of CCC-coated 7075 alloy, sodium saccharin in different concentrations of 0, 0.5, 1 and 1.5 g/l was added to the chromating solution. The coating morphologies for the various GRA concentrations were evaluated by optical microscopy. The optical images of the surface morphologies are shown in Fig. 3. A mud-cracked pattern was formed for all coated samples, independent of the saccharin concentrations. However, found that the extent of cracking increases with increasing concentration of sodium saccharin up to 1.5 g/l. As the coating grain boundaries are commonly preferred sites for cracking, the grain refining role of saccharin results in a higher grain boundary density and therefore enhanced cracking.

Among the variety of suggested mechanisms for coating grain refining,^{32–37} increasing of coating nucleation sites owing to the well-known effect of saccharin in increasing of cathodic overpotential may be considered as an explanation for the CCC grain refining. The energy of grain nucleus formation depends on the cathodic overpotential.^{38–40} A large cathodic overpotential reduces the energy of nucleus formation and hence increases the nucleus density and refines the coating grains. Therefore, the change in the overpotential caused by saccharin

increases the nucleation and reduces the grain size of deposits. The CCC nucleation did not seem to occur at the grain boundaries. However, bridging of the conversion coating across the grain boundaries took place at some locations during coating growth (Fig. 3). A similar observation has been reported by O. Lunder et al.⁹

Figure 4 shows grain size measurements for various concentrations of sodium saccharin. For this measured response, an exponential decrease in grain size was detected with the GRA concentration. After

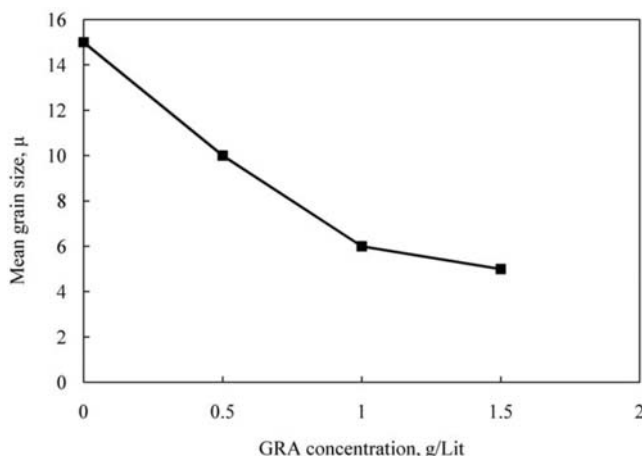


Figure 4. Decrease in grain size of CCCs on the 7075 alloys with GRA (sodium saccharin) concentration.

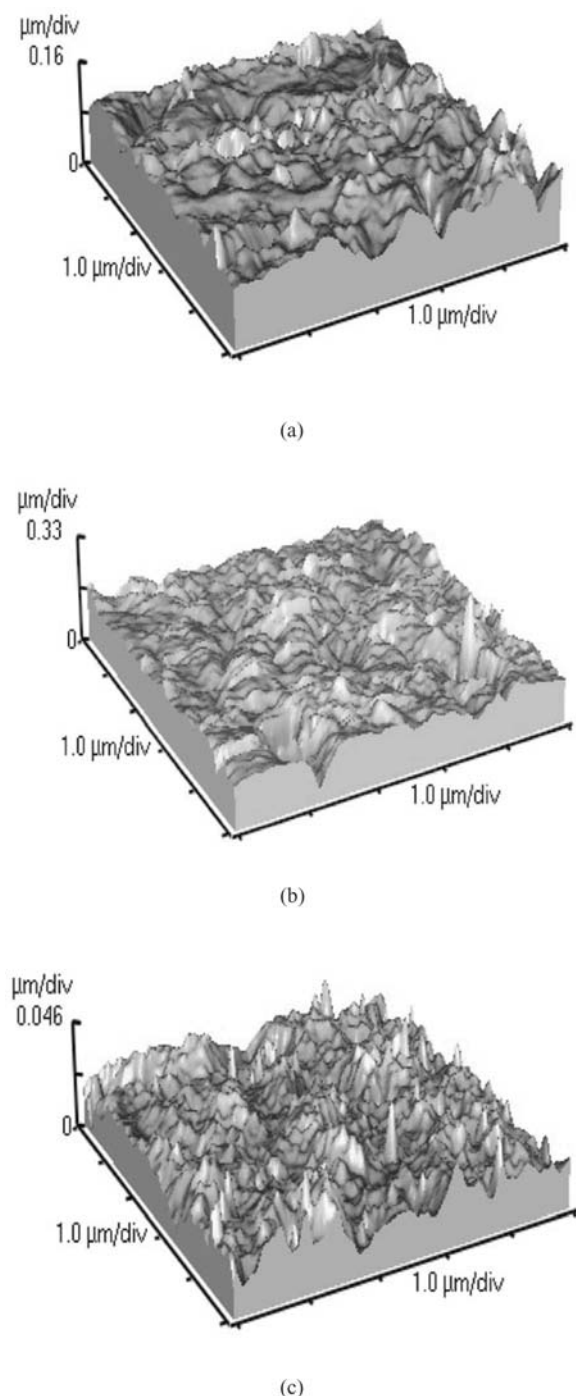


Figure 5. Three-dimension AFM images of CCCs on the 7075 alloys obtained from different immersion times: (a) 30 s, (b) 60 s and (c) 90 s.

major reduction in the coating grain size ($\approx 60\%$) up to 1 g/l of sodium saccharin, a slower decrease was detected. This demonstrated that the grain refining effect of saccharin could be considerable in its medium amount in the chromating solution (i.e. 1 g/l). A further increase in the GRA concentration did not result in significant changes in the coating grain size. This phenomenon can be attributed to the levelling off in the overpotential⁴¹ and/or saturation of adsorption sites on the cathode surface⁴² with increasing saccharin concentration in the bath.

Effect of immersion time.—The 3-dimensional AFM observations show that an increase of the coating immersion time changes the topological morphology of the CCCs formed on 7075 samples. Fig. 5

Table II. RMS values for the chromate conversion coatings formed at different immersion times.

Immersion time (s)	30	60	90
RMS (nm)	46	70	120

demonstrates that the chromate samples for 30 s and 60 s have a more uniform and compact coating structure, while chromating for 90 s forms a coating with nodular texture over most of the surface.

The AFM topographic images were also used to calculate the surface roughness expressed as the root-mean-square (RMS), i.e. the standard deviation of the heights. The RMS results obtained by means of the roughness analysis by WSXM-4 software on the total image of $5 \times 5 \mu\text{m}^2$ are presented in Table II. The small difference in roughness is reasonable, since the CCC film is very thin and hence its surface roughness may vary only to a limited extent. However, the value of RMS increases with immersion time. The change of the immersion time from 30 s to 60 s resulted in an increase of 24 nm in RMS, whereas when the time increased to 90 s the RMS increment was found to be 50 nm. This can be explained by the growth of many more surface asperities (elongated nodules) on the top surface of the 90s-coating (Fig. 5c).

Effect of coating on corrosion resistance.—**Effect of GRA.**—Potentiodynamic polarization scans were performed for all the investigated concentrations of saccharin in the chromating bath. Figure 6 shows anodic polarization curves for CCC-coated samples with saccharin concentrations of 0, 0.5, 1 and 1.5 g/l. From the current density/electrode potential data, the corrosion current density values (i_{corr}) were determined from the Tafel line extrapolation of the anodic i - E curve to the corrosion potential. The i_{corr} and E_{corr} data are summarized in Table III. The corrosion potential became more noble value with increasing of the GRA concentration, indicating a thermodynamic improvement in corrosion resistance as well as better barrier action. This is probably due to the corresponding finer mud-crack morphologies (see Fig. 3) that facilitate the self-healing mechanism.^{43,44} Generally, it is considered that the Cr^{6+} conversion film was consisted of gel-like $\text{Cr}(\text{OH})_3$, which acts as the ‘bone’ framework of the conversion film, and Cr VI compounds, which act as ‘meat’ of the film inside the framework.⁴⁵ As chromate causes self-healing of cracks by migrating from a distance, refining grain size of CCC makes it more compact and more protective. Table III shows that 1 g/l is sufficient concentration when using sodium saccharin as a GRA in the chromating bath for Al 7075 alloy, because it provides about 74 percent reduction in the corrosion rate relative to the free-GRA CCC-coated sample.

Effect of immersion time.—Impedance spectra were collected using the frequency response analyzer after immersion times of 30 s, 60 s and 90 s in the chromating solution. Figure 7 shows the EIS data from all the immersion times plotted in the complex plane. The EIS response of each sample is largely capacitive in all cases, but the

Table III. E_{corr} and i_{corr} values of CCC coatings by different sodium saccharin concentrations in chromating bath.

Saccharin concentration (g/l)	E_{corr} V(SCE)	i_{corr} ($\mu\text{A}/\text{cm}^2$)	Reduction in corrosion rate
0	-0.927	3.8	-
0.5	-0.839	1.5	61%
1	-0.811	1.0	74%
1.5	-0.797	0.9	76%

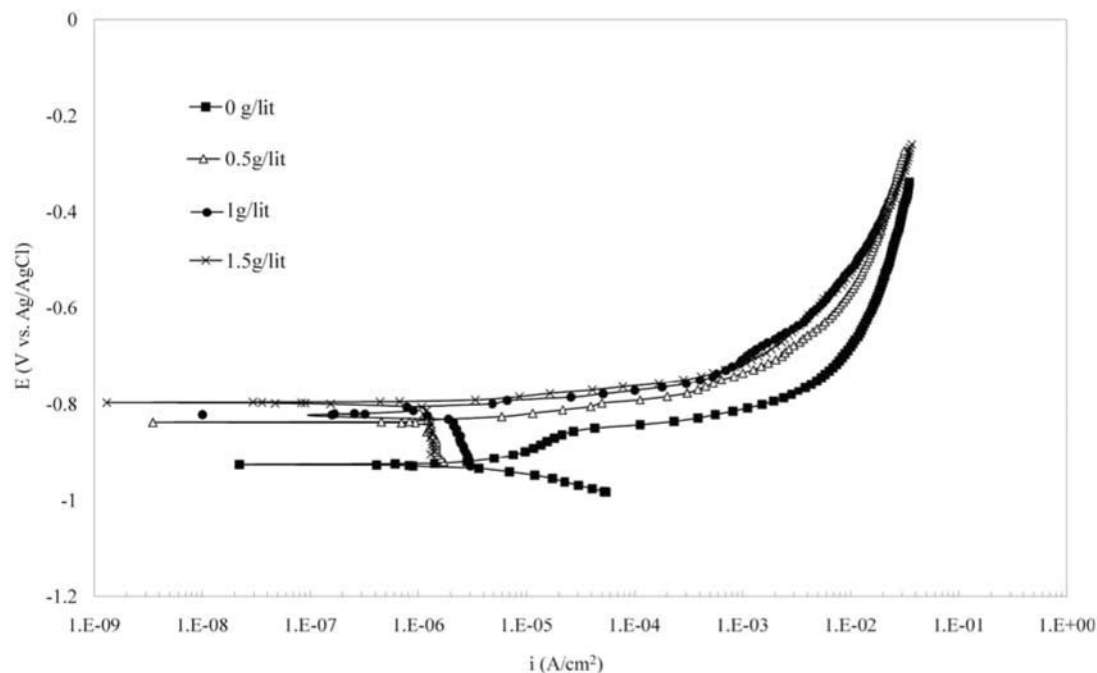


Figure 6. Potentiodynamic polarization curves of the 7075 alloy samples treated in chromating solutions with different GRA (sodium saccharin) concentrations.

effects of immersion time on corrosion resistance (R_{corr}) are easily distinguishable. On average, the R_{corr} for each CCC-coated 7075 is at least about one order of magnitude greater than the untreated alloy. In addition, the corrosion rates of the CCC-coated samples which are in reverse dependence with R_{corr} decreased with immersion time from 30 s to 90 s. This improvement in the corrosion resistance was believed to be related to a thickening of the coating with immersion time. In general, a thicker coating enhances both barrier and self-healing actions of CCCs. In other words, increasing of the insoluble portion of CCC as well as the leachable chromium content in the coating that are expected with increasing immersion time can be considered as two

reasonable explanations for the observed improvement in corrosion resistance of CCC-coated 7075 samples. These characteristics have been supported in other studies.⁴³⁻⁴⁹

The impedance spectra of the 90s-CCC were modelled using an equivalent circuit analysis and complex non-linear least-squares fitting of the data to a suitable equivalent circuit. The equivalent circuit model is shown in Fig. 8. This equivalent circuit was modified from a model used for the oxide film on anodized aluminium.⁵⁰ In this model, CCC is considered to consist of two layers (see Fig. 8): the porous outer layer with many shrinkage cracks and the relative dense inner layer without any cracks that reach the substrate. Figure 9 shows the experimental results and the fitting curves using the equivalent circuit in Fig. 8. A very good fit was obtained, indicating that the equivalent circuit model accurately reflected the coating structures.

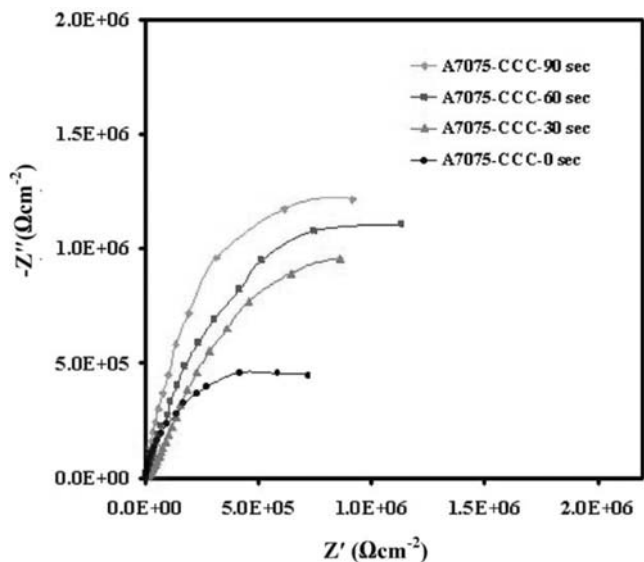


Figure 7. Nyquist plots of the 7075 alloy samples treated in the free-GRA chromating solution in different immersion times.

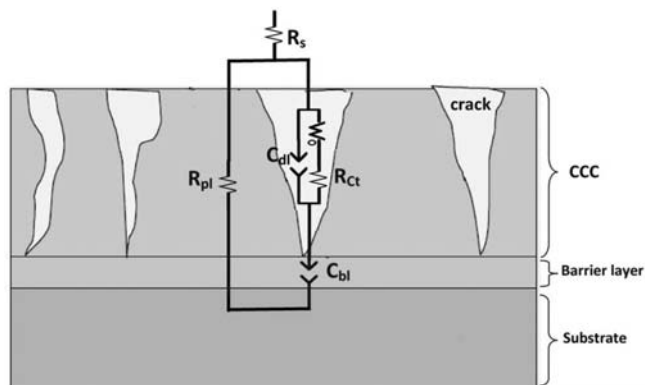


Figure 8. Schematic of cross section of CCC formed after 90 sec immersion time and the equivalently circuit model used to fit impedance spectra. R_{pl} : CCC capacitance, R_s : solution resistance, C_{bl} : Capacitance of $Cr(OH)_3$, C_{dl} : Interfacial capacitance, R_{ct} : Charge transfer resistance.

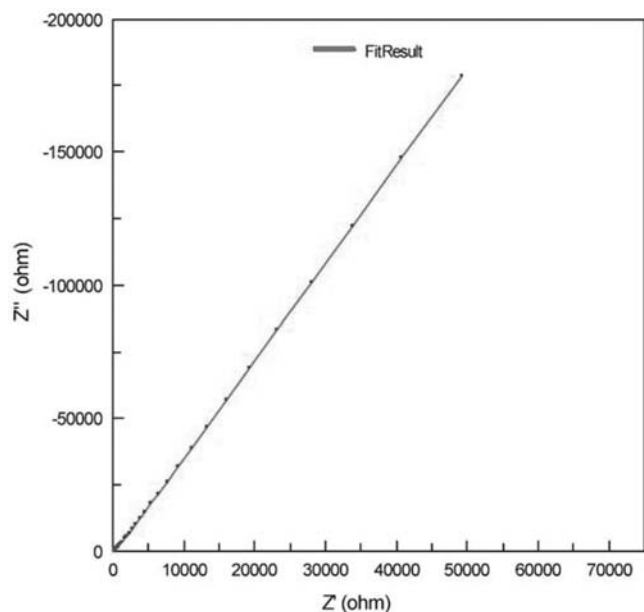


Figure 9. Experimental impedance spectra (dots) of 90 s CCC-coated 7075 alloy and the fitting results (solid line) with the equivalent circuit model in Figure 8.

Conclusions

The results of these experiments and the subsequent discussion support the following conclusions:

- 1) The CCC-coated Al 7075 alloy consisted of two layers: a porous outer layer with many shrinkage cracks (mud-crack morphology) over a thin and relative dense inner layer.
- 2) Very rapid formation of the CCCs (about 0.006 mg s^{-1}) during the short immersion times was observed on 7075 Al alloy. However, nucleation and growth of the CCC was not seen at the alloy grain boundaries even for longer immersion times.
- 3) The CCC roughness increased to a limited nano-scale extent with increasing immersion time.
- 4) The corrosion rates of CCC-coated alloy 7075 decreased with increasing immersion time.
- 5) Sodium saccharin accelerates the CCC nucleation and hence reduces the grain size of the coating deposit. However, a major decrease in the surface grain size of CCCs was observed at a medium saccharin concentration. The same concentration was found to be sufficient to achieve a major reduction in corrosion rate of the CCC-coated alloy 7075.

Acknowledgments

The authors express their sincere thanks to Prof. Robert A. Rapp (Ohio State University) for editing the manuscript.

References

1. D. Zhu and W. J. Van Ooij, *Corros. Sci.*, **45**, 2163 (2003).
2. R. P. Wei, C. M. Liao, and M. Gao, *Metallur. Trans.* **29(A)**, 1153 (1998).

3. R. B. Leggat, S. A. Taylor, and S. R. Taylor, *Colloids and Surfaces*, **210**, 83 (2002).
4. F. W. Lytle, R. B. Gregor, G. L. Bibbins, K. Y. Blohowiak, R. E. Smith, and G. D. Tuss, *Corros. Sci.*, **37**, 349 (1995).
5. A. E. Hughes, R. J. Taylor, and B. R. W. Hinton, *Surf. Interface Anal.*, **25**, 223 (1997).
6. D. Chidambaram, C. R. Clayton, and G. P. Halada, *J. Electrochem. Soc.*, **151**, B151 (2004).
7. J. Zhao, L. Xia, A. Sehgal, D. Lu, R. L. McCreery, and G. S. Frankel, *Surf. Coat. Technol.*, **140**, 51 (2001).
8. P. Campestrini, E. P. M. Van Westing, A. Hovestad, and J. H. W. De Wit, *Electrochimica Acta*, **47**, 1097 (2002).
9. H. S. Isaacs, K. Sasaki, C. S. Jeffcoate, V. Laget, and R. Buchheit, *J. Electrochem. Soc.*, **152**, B441 (2005).
10. P. Campestrini, G. Goeminne, H. Terryn, J. Vereecken, and J. H. W. De Wit, *J. Electrochem. Soc.*, **151**, B59 (2004).
11. G. M. Brown and K. Kobayashi, *J. Electrochem. Soc.*, **148**, B457 (2001).
12. D. Chidambaram, C. R. Clayton, M. W. Kendig, and G. P. Halada, *J. Electrochem. Soc.*, **151**, B613 (2004).
13. W. Zhang, B. Hurley, and R. G. Bunchheit, *J. Electrochem. Soc.*, **149**, B357 (2002).
14. A. Kolics, A. S. Besing, and A. Wieckowski, *J. Electrochem. Soc.*, **148**, B322 (2001).
15. L. Xia and R. L. McCreery, *J. Electrochem. Soc.*, **146**, 3696 (1999).
16. N. Sato, *Corros. Sci.*, **31**, 1 (1990).
17. G. S. Frankel, Air Force Office of Scientific Research, Contract No. F49620-96-1-0479, Final Report (2001).
18. G. Goeminne, Ph.D. Thesis, Vrije universiteit Brussel (1998).
19. N. Le Bozec, S. Joiret, D. Thierry, and D. Persson, *J. Electrochem. Soc.*, **150**, B561 (2003).
20. A. Sehgal, G. S. Frankel, B. Zoofan, and S. Robin, *J. Electrochem. Soc.*, **147**, 140 (2000).
21. K. Asami, M. Oki, G. E. Thompson, G. C. Wood, and V. Ashworth, *Electrochimica Acta*, **32**, 337 (1987).
22. D. Chidambaram, G. P. Halada, and C. R. Clayton, *J. Electrochem. Soc.*, **151**, B160 (2004).
23. W. Zhang, PhD Thesis, Ohio State University (2002).
24. K. Shirvani, *Iranian J. Surf. Eng. (in Persian)*, **6**, 83 (2009).
25. F. W. Eppensteiner and M. R. Jenkind, *Met. Finish.*, **105**, 413 (2007).
26. P. Campestrini, E. P. M. Van Westing, and J. H. W. De Wit, *Electrochimica Acta*, **46**, 2553 (2001).
27. L. Kintrop and L. de Riese-Meyer, and H. KGaA, *Inst. Phys. Cont. Ser.*, **119**, 257 (1991).
28. Q. Meng and G. S. Frankel, *Surf. Inter. Anal.*, **36**, 30 (2004).
29. C. J. Brinker and G. W. Scherer, *Sol-gel science: the physics and chemistry of sol-gel processing*, Academic Press, Boston, MA (1990).
30. J. A. Treverton and M. P. Amor, *Trans. Inst. Met. Finish.*, **60**, 92 (1982).
31. R. A. Dickie, *Progress in Org. Coat.*, **28**, 3 (1994).
32. J. P. Bonino, P. Poudroux, C. Rossignol, and A. Rousset, *Plat. Surf. Finish.*, **79**, 62 (1992).
33. T. C. Franklin, *Plat. Surf. Finish.*, **84**, 62 (1994).
34. D. Mockute and G. Bernotiene, *Surf. Coat. Technol.*, **135**, 42 (2000).
35. A. Ciszewski, S. Posluszny, G. Milczarek, and M. Baraniak, *Surf. Coat. Technol.*, **183**, 127 (2004).
36. B. Szeptycka, *Russ. J. Electrochem. Soc.*, **37**, 684 (2001).
37. Y. Nakamura, N. Kaneko, M. Watanabe, and H. Nezu, *J. Appl. Electrochem.*, **24**, 227 (1994).
38. A. Milchev, *Electrocrystallization: Fundamentals of Nucleation and Growth*, p. 11, Kluwer Academic Publishers (2002).
39. E. Budevski, G. Staikov, and W. J. Lorenz, *Electrochimica Acta*, **45**, 2559 (2000).
40. A. M. Rashidi and A. Amadeh, *Surf. Coat. Technol.*, **204**, 353 (2009).
41. C. C. Roth and H. Leidheiser, *J. Electrochem. Soc.*, **100**, 553 (1953).
42. J. Edwards, *Trans. Inst. Met. Finish.*, **41**, 169 (1964).
43. J. Zhao, G. S. Frankel, and R. L. McCreery, *J. Electrochem. Soc.*, **145**, 2258 (1998).
44. M. W. Kendig, A. J. Davenport, and H. S. Isaacs, *Corros. Sci.*, **34**, 41 (1993).
45. G. Meng, L. Zhang, Y. Shao, T. Zhang, F. Wang, C. Dongc, and X. Li, *Scrip. Material.*, **61**, 1004 (2009).
46. I. Suzuki, *Corrosion Resistant Coatings Technology*, Marcel Dekker Inc., New York, (1989).
47. T. Biestek and J. Weber, translated from the Polish by A. Kozlowski, *Electrolytic and Chemical Conversion Coatings*, Portcullis Press Limited-Redhill, Poland (1976).
48. W. E. Pockock, *Met. Finish.*, **52**, 48 (1954).
49. E. Akiyama, A. J. Markworth, J. K. McCoy, G. S. Frankel, L. Xia, and R. L. McCreery, *J. Electrochem. Soc.*, **150**, B83 (2003).
50. J. Hitzig, K. Juttner, W. J. Lorenz, and W. Paatsch, *Corros. Sci.*, **24**, 945 (1984).